Influence of Polycarbonate Flexibility on the Annealing Induced Phase Separation in the Hole Transport Molecule TPD in a Model Charge Transport Composite

ARTICLE *in* THE JOURNAL OF PHYSICAL CHEMISTRY B · JANUARY 2004

Impact Factor: 3.3 · DOI: 10.1021/jp036306k

3 AUTHORS, INCLUDING:

Ferdous Khan
KNAUF INSULATION LTD.
47 PUBLICATIONS **580** CITATIONS
SEE PROFILE

Pudupadi R Sundararajan
Carleton University
127 PUBLICATIONS **2,240** CITATIONS
SEE PROFILE

Influence of Polycarbonate Flexibility on the Annealing-Induced Phase Separation of the Hole Transport Molecule TPD in a Model Charge Transport Composite

Ferdous Khan, Ah-Mee Hor,† and P. R. Sundararajan*

Department of Chemistry, Carleton University, 1125 Colonel By Drive, Ottawa, Ontario K1S 5B6, Canada

Received: August 5, 2003; In Final Form: October 15, 2003

The depression of glass transition temperature, annealing-induced phase separation, and morphology were investigated in a binary solid solution of *N*,*N*′-diphenyl-*N*,*N*′-bis(3-methylphenyl)-[1,1′-biphenyl]-4,4′-diamine (TPD) in bisphenol A polycarbonate (BPAPC) and cyclohexyl polycarbonate (PCZ) with three different molecular weights. Differential scanning calorimetry, X-ray diffraction, microscopy, and FTIR were used to characterize these composites. Molecularly doped TPD in polymers significantly depressed the T_g of the host polymers. Although it could be expected that the TPD would disperse well in a flexible polymer and cause a substantial decrease in T_g, we find that the extent of depression is more pronounced with the rigid polymer. FTIR studies indicate that a molecular level interaction exists between TPD and the polycarbonates, as shown by the frequency shifts in the aromatic region. Upon annealing, the phase separation and crystallization of TPD lead to a recovery of the T_g of the polymer, by 10−20 °C, depending on the temperature and time of annealing. In the case of TPD/BPAPC composites, although the crystallinity of the phase-separated TPD was found to be close to 30%, the extent of recovery of the T_g was small. This is attributed to the plasticizing effect of the TPD crystals. A lower degree of crystallinity was observed in the case of TPD/PCZ, which is due to the lower molecular flexibility of the PCZ relative to BPAPC as well as the difference between the T_g of the polymer and the annealing temperature. The molecular weight and its dispersion has a significant effect on the recovery of the T_g in the case of PCZ, as well as the crystallinity of the phase-separated TPD.

Introduction

Organo-electronic devices such as photoreceptors, organic light emitting diodes (OLED), and electrochromic devices are generally multilayer composites. Such organic devices are normally prepared as a binary solid solution, consisting of charge transporting donor or acceptor molecules dispersed in a polymer binder. In commercial applications, such "molecularly doped" systems are preferred to polymers bearing the active moieties on the backbone or the side chain because the concentration of the active component can be changed at will.[1,2] It is generally agreed that the charge transport occurs by a hopping mechanism, and hence the dispersion of the active molecule and the intermolecular distance become important.[2−4] The hole transporting molecule, *N*,*N*′-diphenyl-*N*,*N*′-bis(3-methylphenyl)[1,1′-biphenyl]-4,4′-diamine (TPD), is known to be an electron donor and is employed in organic photoreceptors in the charge transport layer (CTL)[1]. Though polycarbonate (PC) is generally used as the binder polymer, the effect of several types of polymer binders on the charge mobility has been studied[2,5−9] to demonstrate that the binder does have an influence on the properties of the CTL. Higher charge mobility has been found in the case of TPD/polystyrene film in comparison to the TPD/PC films. Yuh and Pai[7] and Mishra et al.[10] showed that the mobility remains almost steady for both TPD/ phenoxy and TPD/polystyrene films with the increase of electric field, whereas it was dependent on the electric field in the case of the TPD/PC film. The luminescence properties of these systems have been studied by several authors.[11−16]

Stolka et al.[2,17,18] investigated films of solid solutions of TPD in bisphenol A polycarbonate with different concentrations and found no crystallization of the TPD at room temperature up to 80%. A high concentration of TPD in the polymer host is preferred because the charge mobility usually increases with the concentration of charge transport molecules as the intermolecular distance between them is decreased.

Recently, Santerre et al.[19] reported the properties of OLED devices based on TPD dispersed in polymers with high T_g. The best performance was obtained with a TPD concentration of 75%. The typical thickness of the hole transport layer was 80 nm, whereas in the CTL of the photoreceptors, the thickness is in the range of 10−40 μm.[1]

It was mentioned above that the intermolecular distance between the dispersed active molecules plays a role in the functional properties of the device. However, any phase separation of the active molecule would lead to its crystallization and deterioration of the device performance. Using solid-state NMR studies of TPD-PC composites, Kaplan[20] concluded that attractive interaction exists between the polymer and the TPD in this system. He also noted that phase separation and crystallization of the TPD would occur if the sample were annealed at temperatures close to the T_g of the host polymer.

The phase separation of the hole transport molecule is of important consequence, especially in devices such as the OLED, due to the heat generated during the functioning of the device. Smith et al.[21] have shown that crystallization of the TPD was the cause of delamination of an OLED device. The crystallization would also lead to charge trapping. Scharfe[22] has discussed the effect of charge trapping, its build up with each cycle of charging of the photoreceptor, and the resultant increase in the

* Corresponding author. E-mail: Sundar@Carleton.ca.
† Xerox Research Centre of Canada, 2660 Speakman Drive, Mississauga, Ontario L5K 2L1 Canada.

10.1021/jp036306k CCC: $27.50
Published on Web 11/27/2003

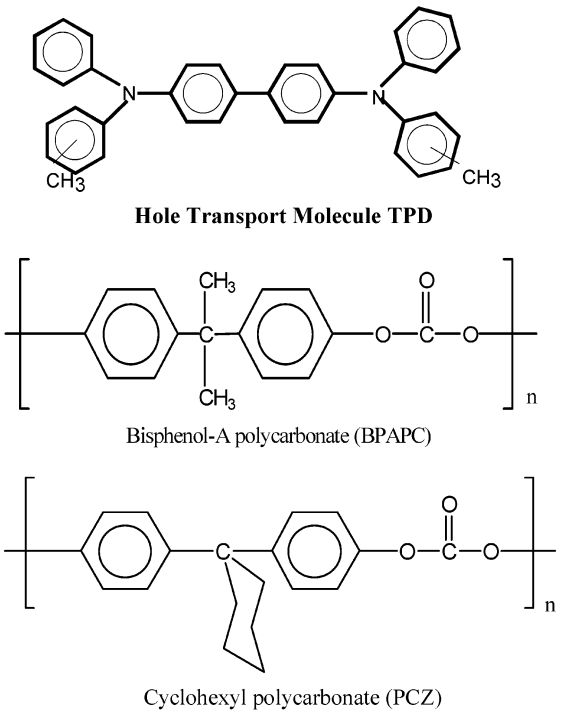

Figure 1. Schematic of the chemical structures of TPD, bisphenol A polycarbonate (BPAPC) and cyclohexyl polycarbonate (PCZ).

residual voltage that would cause print defects. The phase separation of the TPD would also depend on the type of the host polymer, and its T_g.

Although it is recognized that the crystallization of TPD leads to charge trapping in photoreceptors and to delamination in the case of, e.g., OLED devices, a systematic study of the phase separation from the polymer host has not been reported. In this paper, we describe our studies on the phase separation induced by annealing of films containing TPD and two different types of polycarbonates. One of them is the bisphenol A polycarbonate (denoted as BPAPC) and the other, three samples of cyclohexyl polycarbonate (denoted as PCZ). The PCZ polycarbonate has a higher T_g than BPAPC, in the range 160−180 °C, depending on the molecular weight. We chose these two polycarbonates to compare the influence of conformational flexibility, because they differ only by the substitution on the isopropylidene carbon. In addition, the BPAPC and the PCZ polycarbonates are most commonly claimed in patents for use in photoreceptor devices.[23−25] Previous molecular modeling studies[26,27] showed that the chain flexibility of PCZ is more restricted than that of the BPAPC and the conformational entropy is lower. The conformational flexibility of the binder polymer could contribute to the extent of crystallization of the TPD. Techniques such as the DSC, X-ray diffraction, polarizing optical microscopy, and FTIR were used in the current study. Annealing temperatures in the range 120−140 °C were used[20] for varying lengths of time. Below this temperature range, no significant crystallization occurs. We will discuss the differences and similarities between TPD-BPAPC and TPD-PCZ systems, the latter being with the polymer that is conformationally more rigid than BPAPC. The difference between the annealing temperature and the T_g affects the extent of crystallization of the TPD.

Experimental Section

The molecular structures of TPD, BPAPC, and PCZ are shown in Figure 1. These materials were courtesy of Xerox Research Centre of Canada. The M_w and the polydispersity, as measured by GPC are given in Table 1. Coating solutions were prepared by dissolving appropriate mixtures of TPD and the polymers in dichloromethane of laboratory grade. Concentrations of 40 and 50% (wt) of TPD in the polycarbonates were used. Films were coated on glass substrate using an electrically driven film coater and these were then dried at a very low rate of the solvent evaporation at ambient conditions for at least 48 h. The final thickness of the films was about 10−15 μm. Samples were annealed using a vacuum oven with an accuracy of ±1 °C at different temperatures and times.

TABLE 1: Molecular Weight and T_g of Polycabonates Used in This Study and Their Films with TPD

sample	M_w	poly-dispersity	T_g (°C) (onset)	T_g (°C) (midpoint)
BPAPC	250 860	1.75	148	154
TPD/BPAPC: 40/60			85.3	97.3
TPD/BPAPC: 50/50			69.8	80.6
PCZ-1	55 400	3.3	167.7	176.3
TPD/PCZ-1: 40/60			65.2	71.3
PC Z-2	112 800	4.4	174.6	182.2
TPD/PCZ-2: 40/60			75.1	86.2
TPD/PCZ-2: 50/50			71.0	83.2
PCZ-3	365 500	1.81	178.6	184
TPD/PCZ-3: 40/60			86.0	103
TPD/PCZ-3: 50/50			82.0	96.4

Thermal analysis was performed using a DuPont 910 differential scanning calorimeter (DSC) at a heating rate of 10 °C/min. The DSC instrument was calibrated for temperature and energy with indium and tin reference samples. DSC traces were recorded with about 8−10 mg of sample, in a nitrogen atmosphere. The crystallinity of the samples was calculated as the ratio of the measured heat of fusion of the composite film corresponding to the melting endotherm of TPD (normalized to the weight fraction of TPD in the sample), and the heat of fusion of 100% crystalline TPD. In the discussion that follows, the onset T_g is used.

X-ray diffraction data were collected using a Philips automated powder diffractometer Model PW 1710. Nickel-filtered Cu Kα radiation (λ = 1.54 Å) was used. The MDI Data Scan 3.2 software (Materials Data Inc., Livermore, CA) was used for data collection. The results were analyzed using MDI Jade 5, to determine the crystallinity (X_c). X_c was calculated as the ratio of the intensity under the crystalline peaks above the background to the total intensity. A Zeiss Axioplan polarizing optical microscope was used to record optical micrographs. The Northern Eclipse software was used for image analysis.

Fourier Transform infrared (FTIR) spectroscopic measurements were carried out at ambient conditions using a Michelson M129 BOMEM FTIR spectrometer. All the data were collected using BOMEM GRAMS/386 software. The FTIR spectrum of TPD was obtained by preparing the sample in the form of a transparent KBr pellet. The FTIR spectra of polymer and composite films were taken using a NaCl disk. A background FTIR spectrum was taken for each experiment with the identical sample holder.

Simple molecular modeling was performed using the HyperChem software (ver 6.01).

Results and Discussion

Depression of the Glass Transition Temperature. Differential scanning calorimetry (DSC) analysis of TPD showed an endothermic peak at about 171 °C with a heat of fusion 17.78 cal g^{-1}. The glass transition temperatures of the films of BPAPC and PCZ are given in Table 1.

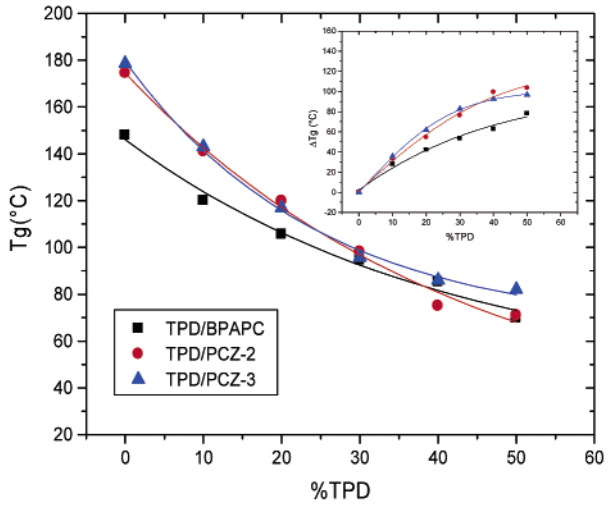

Figure 2. The variation of T_g of the polycarbonates (BPAPC, PCZ-2, and PCZ-3) with different concentrations of TPD. The inset shows the depression ΔT_g of the T_g.

As expected, the T_g of the polycarbonate was depressed by the addition of TPD. In the examples discussed here, we observe a single glass transition temperature, and no transition is observed at higher temperatures that could be attributed to the polymer matrix. No distinct transition is observed that could be assigned to TPD. As prepared, the films (blends) are homogeneous. Thus, the depression of the T_g's is attributable to the effect of addition of the TPD. The variation of T_g of BPAPC, PCZ-2 and PCZ-3 with the concentration of TPD is shown in Figure 2 and Table 1 for the as-prepared films. The depression of the T_g, i.e.,

$$\Delta T_g = T_g\,(\text{polycarbonate}) - T_g\,(\text{composite}) \qquad (1)$$

is also shown in this figure. With 50% TPD, the T_g of BPAPC is reduced to as low as 70 °C. Discussion in this article will be limited to 40 and 50% concentrations of TPD, as these compositions are relevant to device applications. We express the compositions of the composites in terms of weight percent, which is a common practice for investigations related to these types of devices. For conversions of these to the molar volume, note that the molecular weight of TPD is 516.66, which is twice that of the repeat unit of BPAPC (254.27). The molecular weight of the repeat unit of PCZ is 294. The TPD crystallizes[28] with the $P2_12_12_1$ symmetry, and the density is 1.202 g cm^{-3}. The reported[29] density of BPAPC is 1.2 g cm^{-3}.

The T_g of the BPAPC is depressed by 63 deg with 40% TPD and by 78 deg with 50%. Additionally, a small endothermic peak was observed at 166 °C with the film with TPD/BPAPC: 50/50, which is attributed to the melting of the TPD. This indicates that the T_m of the TPD is depressed by about 5 deg, in the presence of BPAPC. Similar depression of the T_m of the small molecule has been noted in the case of diphenyl terephthalate and diphenyl isophthalate dispersed in poly-(styrene-*co*-*n*-butyl acrylate),[30] a liquid crystalline polymer[31] and in BPAPC.[32]

The T_g's of the PCZ-1, PCZ-2, and PCZ-3 samples are 168, 175, and 179 °C, respectively, as listed in Table 1. It is seen from Figure 2 that in the presence of TPD, the depression of the T_g of PCZ is much more pronounced than in the case of BPAPC. With a 40% concentration of TPD in PCZ-1, a T_g of 65 °C was observed (Table 1). This is a reduction of 103 deg. With the same concentration of TPD, the T_g's of PCZ-2 and PCZ-3 were reduced by 100 and 93 deg, respectively. With a

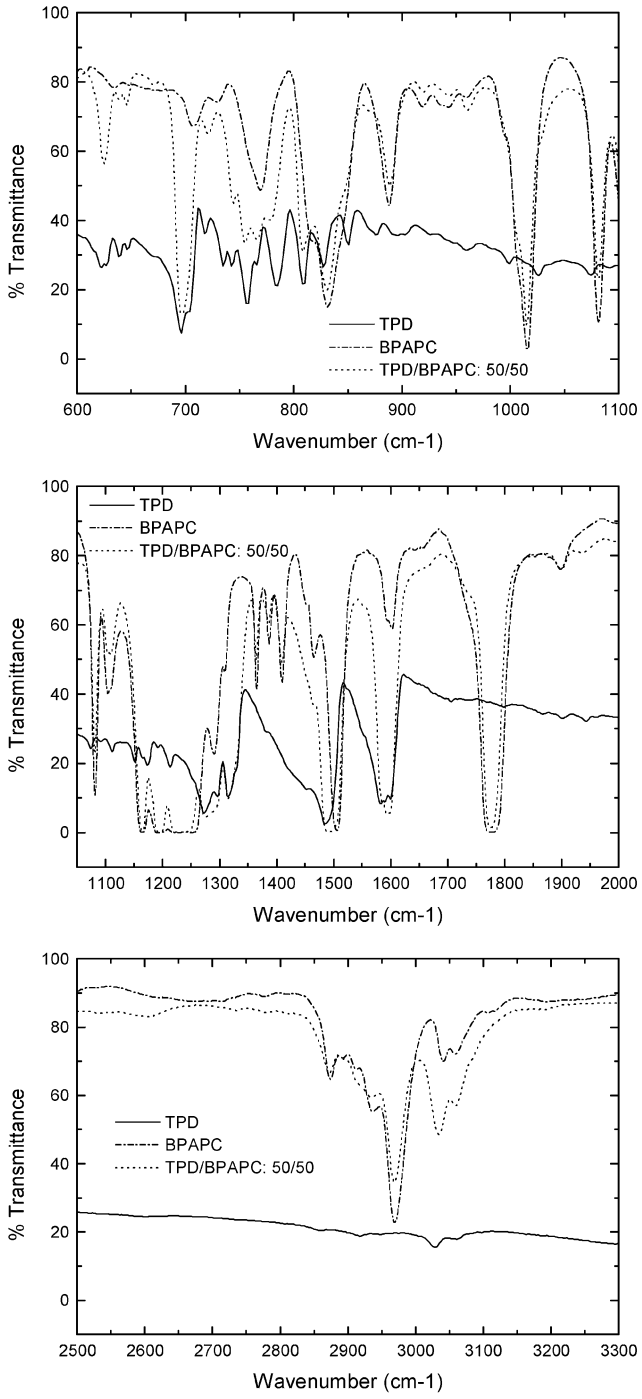

Figure 3. FTIR Spectra of TPD, BPAPC, and TPD/BPAPC:50/50% film.

TPD concentration of 50%, the reduction in T_g is slightly higher (Table 1). Such a concomitant decrease, by as much as 150 deg, in T_g was noted by Santerre et al.,[19] when the TPD was mixed with a poly(aryl ether ketone) with a T_g of 252 °C. It should be mentioned that such a depression of T_g in these cases is not due to residual solvent.

The extent of reduction of T_g with the concentration of TPD depends on the type of polycarbonate. For each of the compositions, the depression of the T_g is higher with PCZ than with BPAPC. It is known[26,27] that PCZ is conformationally more restricted than BPAPC. In the latter, synchronous rotation of the contiguous phenyl groups leads to a range of conformations accessible to the chain. In the case of PCZ, however, the accessible conformations are limited, and such synchronous

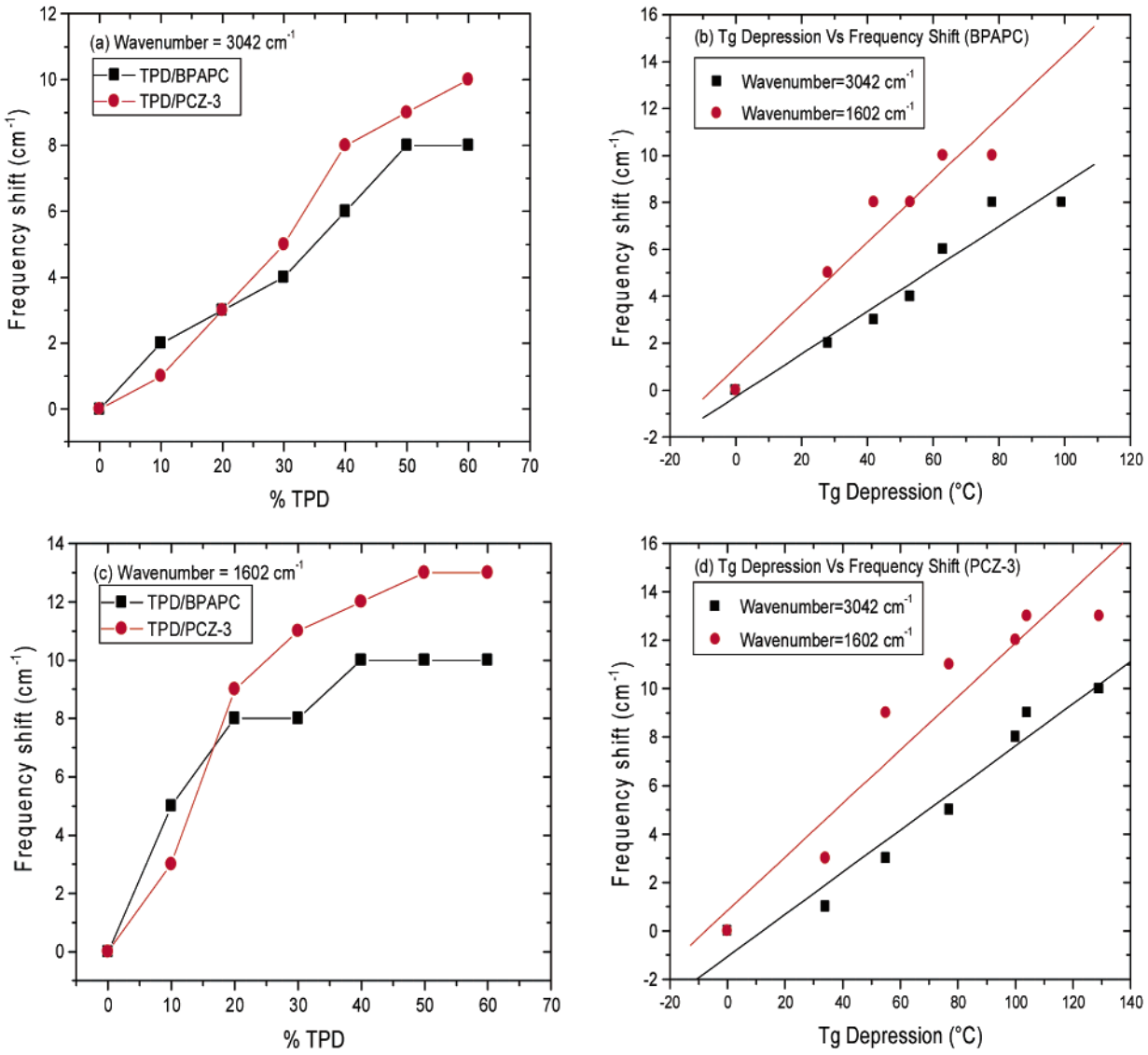

Figure 4. (a) and (c) variation of the frequency with the concentration of TPD in polycarbonates BPAPC and PCZ-3, for the bands at 3042 and 1602 cm^{-1}. (b) and (d) correlation between the T_g depression (ΔT) and frequency shifts.

rotations are impeded (compare Figures 2 and 8 of ref 26). The conformational partition function was calculated[26] to be 179.3 for BPAPC and 40 for PCZ. The ^{13}C spin−lattice relaxation measurements[33] showed that the fast component contribution (due to π flipping phenyl groups) of the T_1 relaxation time is 68% with BPAPC and 42% with PCZ. This indicates the restriction to phenyl motion in the latter. One would expect that the TPD would disperse more efficiently with the more flexible BPAPC and lead to a higher reduction in the T_g. On the contrary, it is seen that the higher the rigidity (higher the T_g) of the host polymer, the larger the reduction in T_g. The addition of the small molecule is expected to increase the free volume of the polymer and thus depress the T_g. It appears that the free volume created by TPD is significant in the case of PCZ. Even with PCZ, the reduction in T_g with 40% TPD is 103 deg for PCZ-1 and it is 93 deg in the case of PCZ-3. We attribute this higher reduction with PCZ-1 relative to PCZ-3, to its lower molecular weight and higher polydispersity, which would facilitate intercalation of TPD. The M_w of BPAPC and PCZ-3 are of the same order.

The effect of diluents on the T_g of the polymers has been described by equations such as those of Kelley and Bueche[34] or Couchman and Karasz[35] using free volume theories. However, application of these equations to the present case requires the knowledge of the coefficient of cubic expansion of TPD or the change in the heat capacity at the T_g of the diluent. These data are not readily available. We tried to fit the results to the simple Fox equation.[36] Values of 61 and 65 °C have been reported for the T_g of TPD.[37,38] Using an average of 63 °C for TPD, a T_g of 374K (101 °C) is obtained for the 50/50 wt % composition of TPD and BPAPC, which is significantly higher than the experimental value of 70 °C. Similarly, for the same composition with PCZ-3, the calculated T_g is 385 K (112 °C), again much higher than the experimental value of 82 °C. We believe that such a discrepancy, i.e., the results of experiments being lower than the theoretical values, is due to specific interactions that exist between the polycarbonates and the TPD, as indicated by IR spectra (see below). This would mean that the reduction of T_g by TPD is not only due to contribution to the change in the free volume, but due to the molecular interaction mentioned above.

Change in free volume can occur on more than one length scale. For example, in the absence of specific interactions, the diluent could intercalate in domains of the polymer that are on the scale of several nanometers (e.g., the usual long spacings or domain sizes (∼50−100 nm) measurable by small angle scattering techniques). A typical example is the solvent induced

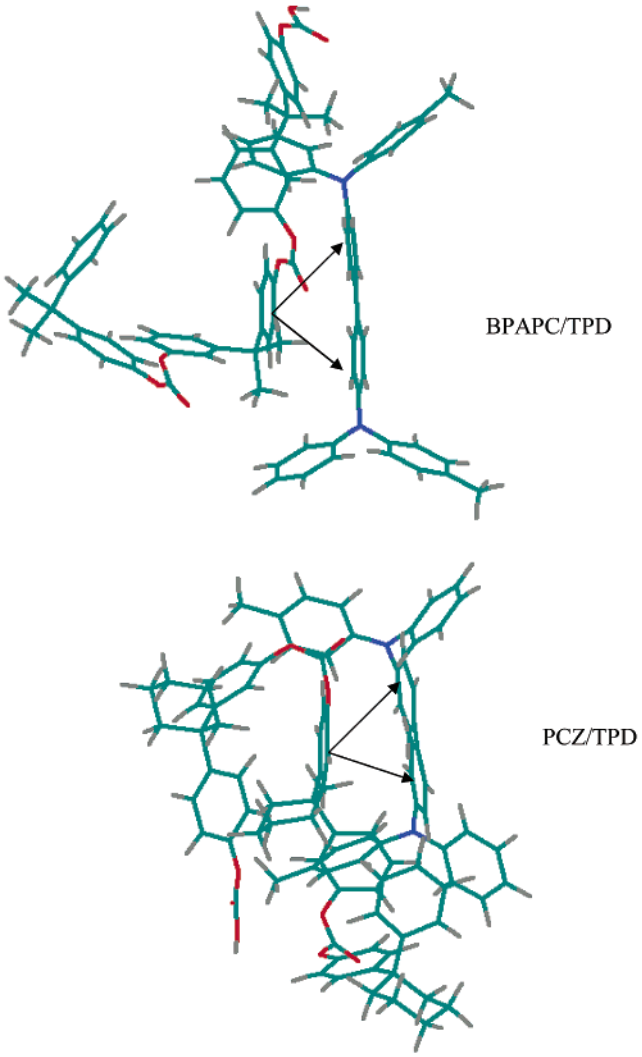

Figure 5. Conformations of the TPD/BPAPC (top) and TPD/PCZ pairs, showing the aromatic overlap of the biphenyl segment of TPD and the phenyl group of the polycarbonate.

crystallization, where the diluent need not be a good solvent for the polymer. If there is a specific interaction between the polymer and the diluent on the molecular scale, the change in the free volume could be more significant due to the intercalation of the diluent at the molecular scale (angstrom scale) rather than at the domain level. It should be noted that concentrations of 50% (wt) of TPD could be incorporated in the BPAPC and PCZ polycarbonates. On the other hand, common plasticizers, such as diphenyl terephthalate, would phase separate beyond a concentration of about 15%. Thus, a higher depression of T_g could be expected when there is a specific interaction between the TPD and the polycarbonate. This is discussed below on the basis of FTIR results and molecular modeling.

The studies of Kaplan[20] using solid-state NMR methods showed molecular level interaction between TPD and BPAPC. The FTIR results also indicate such molecular level interaction between the TPD and the polycarbonates. Previous FTIR studies[39,40] on BPAPC polycarbonate were mainly concerned with the conformation of the carbonate segment (1775−1223 cm^{-1} region of the spectrum), in particular the trans−trans to trans−cis transition.

The frequency shifts of some of the peaks in the aromatic region of the FTIR spectra follow the same trend as the T_g depression. Figure 3 shows the FTIR spectrum of TPD/BPAPC (50:50) composite film along with the spectra of pure TPD and

TABLE 2: Glass Transition Temperatures (°C) of the Various Composites after Annealing for Different Times

	annealing temp (°C)			annealing temp (°C)		
time (h)	120 °C	130 °C	140 °C	120 °C	130 °C	140 °C
	TPD/BPAPC: 40/60 wt %			TPD/BPAPC: 50/50 wt %		
0	85.3	85.3	85.3	69.8	69.8	69.8
0.5	86.3	87.0	87.5	77	77.5	78.1
1	86.5	88.0	88.1	78.3	79	79.7
2	87.3	88.0	89.1	78.5	79.1	79.7
3				78.8	79.2	81.4
4	88.5	89.5	90.4	79.0	80.1	81.3
	TPD/PCZ-1: 40/60 wt %					
0	64.5	64.5	64.5			
0.5	84.0	85.0	86.0			
1	85.8	87.5	88.0			
2	86.5	87.0	89.1			
4	86.8	88.0	89.0			
	TPD/PCZ-2: 40/60 wt %			TPD/PCZ-2: 50/50 wt %		
0	75.1	75.1	75.1	71.0	71.0	71.0
0.5	86.0	87.0	88.5	76.1	77.5	78.0
1	87.7	88.9	89.0	82.5	83.0	86.0
2	89.5	89.8	90.0	83.9	84.6	88.5
4	89.0	90.0	91.0	84.0	85.0	88.3
	TPD/PCZ-3: 40/60 wt %			TPD/PCZ-3: 50/50 wt %)		
0	85.0	85.0	85.0	81.9	81.9	81.9
0.5	90.0	90	90.4	83	83.1	83.4
1	91.2	92.0	91.8	83.5	84.2	85
2	92.6	93.9	94.9	86	87	87.5
4	94.5	95.1	96.0	87	87.5	88.5

BPAPC film. The bands at 1602 and 1505 cm^{-1} in the BPAPC spectrum correspond to the para aromatic ring stretch.[29,41] These bands shift to lower frequencies by 8 and 15 cm^{-1}, respectively, in the TPD/BPAPC spectrum. The peaks in the region 3000−3200 cm^{-1} correspond to aromatic CH stretches. The peak at 3041 cm^{-1} in the BPAPC spectrum shifts to lower frequency, by 6 cm^{-1}, in TPD/BPAPC. In addition, new peaks appear at 2934 and 3059 cm^{-1} in the latter. The BPAPC absorption band at 707 cm^{-1}, assigned to the CH out of plane vibration of the aromatic ring is shifted by 10 cm^{-1}, with much higher intensity, in the spectrum of the composite. The changes in the spectra of the TPD/PCZ are similar to those found with BPAPC.

Figure 4 shows the effect of the concentration of TPD on the shift in the frequencies of the aromatic CH stretch and the aromatic ring stretch. With 50−60% TPD, both absorption peaks shift by 8−10 cm^{-1} with BPAPC, and 10−13 cm^{-1} in the case of PCZ-3. It is seen from Figure 4a,c that beyond a TPD concentration of about 20%, the frequency shifts are higher with PCZ. These frequency shifts indicate specific interactions between the aromatic groups of the polycarbonate and the TPD, i.e., the alignment of the segment of the TPD with the phenyl groups of the polycarbonates.

Also plotted in Figure 4 is the frequency shift as a function of the ΔT_g, the extent of depression of T_g with the concentration of TPD. Although the depression of the T_g would be due to a combination of factors such as the molecular interaction, change in the free volume of the polymer, etc., it is interesting that the IR frequency shifts follow the same trend with the concentration of the TPD.

To confirm the possibility of the aromatic interaction, a simple molecular modeling was performed. Using the HyperChem software, models of TPD, and trimers of BPAPC and PCZ were energy minimized. Pairs of TPD/BPAPC and TPD/PCZ were then created by placing the TPD molecule in proximity of the polycarbonates. The pairs were then energy minimized. Relatively, the energies of the TPD, and the trimers of BPAPC and

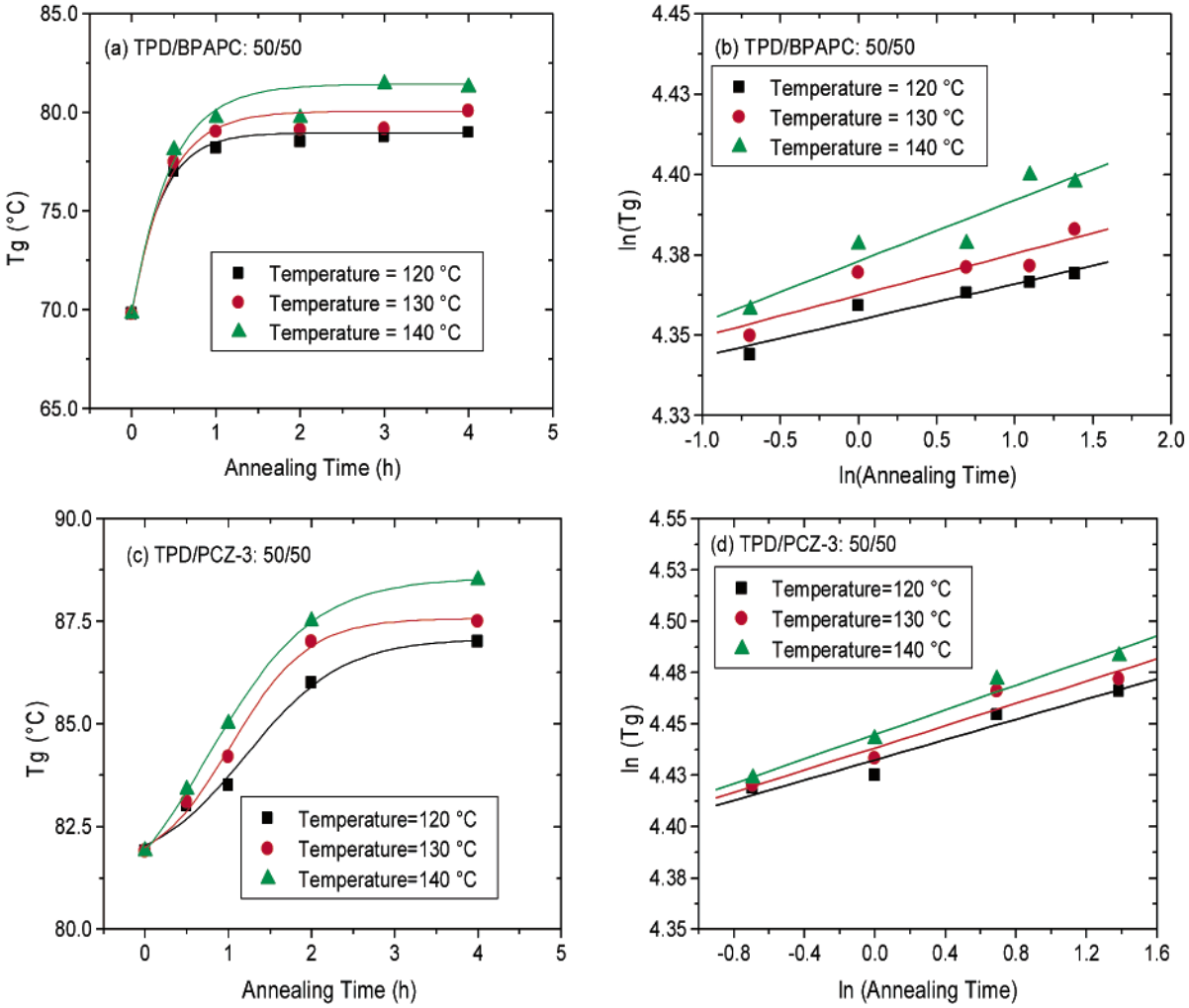

Figure 6. Glass transition temperature (T_g) versus annealing time of (a), (b) TPD/BPAPC (50:50 wt %) and (c), (d) TPD/PCZ-3 (50:50 wt %) films, at 120, 130, and 140 °C. (b) and (d) are shown as ln−ln plots.

PCZ were 16.3, 18.1, and 39 kcal mol^{-1} respectively. (Previous molecular mechanics calculations[26] showed that the minimum energy conformation of the PCZ monomer was higher in energy by 5.3 kcal mol^{-1} than that of BPAPC. Hence, the difference of about 21 kcal mol^{-1} between the energies of trimers of BPAPC and PCZ is reasonable.) The energy of the TPD/BPAPC and TPD/PCZ pairs reduced to 5.4 and 16.3 kcal mol^{-1}, respectively. The extent of lowering of the energy is thus about 13 and 23 kcal mol^{-1}, respectively, for the TPD/BPAPC and TPD/PCZ pairs, relative to the energy of the individual polymers. The larger depression of the T_g of PCZ compared to BPAPC accords with the larger decrease in energy in the case of the TPD/PCZ pair. The conformations of the pairs are shown in Figure 5. It is seen that in both cases, the biphenyl segment of TPD overlaps with one of the phenyl groups of the polycarbonate. The distance between the overlapping aromatic groups is about 3.8 Å, which is the characteristic π overlap distance. This overlap involves the biphenyl segment of the TPD rather than the one of the diphenyl side groups.

Recovery of the T_g. Annealing these films at different temperatures results in crystallization of TPD to varying degrees. The higher T_g and the more restricted chain flexibility of PCZ lead to different phase separation behavior, whereas the annealing is performed at the same temperatures. Upon the crystallization of the TPD, the T_g of the polycarbonate is partially recovered, the extent of recovery depending on the temperature and time of annealing and the concentration of the TPD. With the crystallization of the TPD (see next section), there would be a depletion of the small molecule in the polymer matrix and this leads to the recovery of the T_g of the host matrix. The results are given in Table 2. As a graphical illustration, the recovery of T_g with annealing time is shown in Figure 6, for temperatures 120, 130, and 140 °C, for 50% concentration of TPD in BPAPC and PCZ-3. With a TPD concentration of 40%, the T_g recovery is rather small (Table 2). Figure 6a shows that the increase in T_g is sharp during the first thirty minutes with 50% TPD, and levels off. Beyond 2 h, no further significant increase is observed. For the TPD/BPAPC: 50/50 film, annealing at 120 °C for 3 h increases the T_g from 70 to 79 °C, and at 140 °C, to 81 °C. Thus in this case, the difference in the T_g recovery is not pronounced when the annealing temperature is increased by 20°. In all these cases, the onset T_g is given. In most cases of the annealed films, the glass transition is broad, and determining the midpoint T_g was difficult. Examples of the difference between the temperature range of the transitions in the as prepared and annealed films are shown in Figure 7. It is seen that the transitions are broader in the case of the annealed films, due to the inhomogeneity resulting from the annealing.

The change in the T_g of PCZ-3, with 50% TPD is gradual, as shown in Figure 6c, in contrast to the sharp change during annealing for an hour for BPAPC. Parts b and d of Figure 6 show the change in T_g as a ln−ln plot with annealing time. In each case, the slopes of the curves for 120, 130, and 140 °C are similar. Ideally, these should be superimposable with a shift

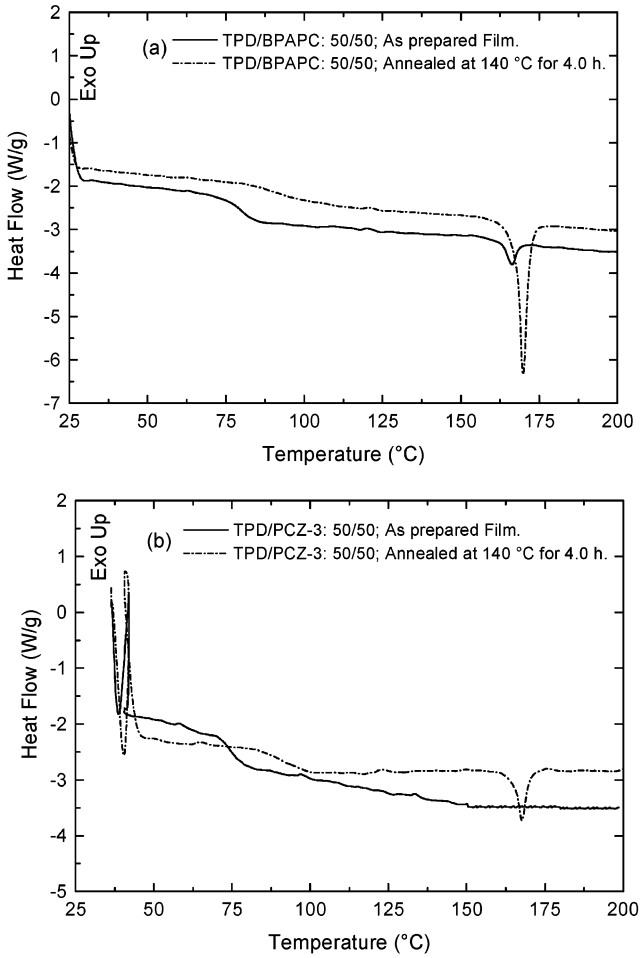

Figure 7. DSC traces of (a) TPD/BPAPC and (b) TPD/PCZ-3 composites as prepared and after annealing at 140 °C for 4 h.

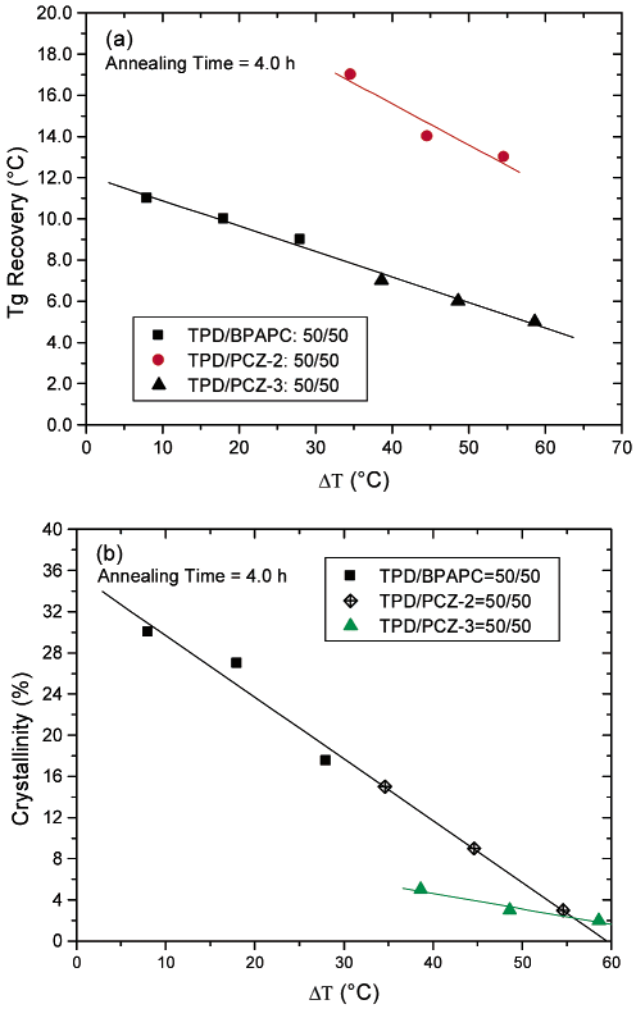

Figure 8. T_g recovery (a) and the DSC crystallinity (b), plotted as a function of the difference (ΔT_{ann}) between the T_g of the polymer and the annealing temperature.

factor. The rate of change of T_g with time is similar for the temperatures used here.

With the TPD/BPAPC composites, with 40% TPD, there is a T_g recovery of about 5 deg upon annealing, and it is 10 deg with a concentration of 50%. This is slightly higher relative to the TPD/PCZ-3, as seen from Figure 6 and Table 2. The effect of molecular weight and the polydispersity in the case of PCZ is evident from the results shown in Table 2. It is seen that even with 40% TPD, the PCZ-1 shows a T_g recovery of 25 deg (upon annealing at 140 °C for 4 h). This is 2−3 times larger than the recovery noted in the case of BPAPC composites. The film with 50% concentration of TPD with PCZ-1 was very brittle, and no further analysis was undertaken with this composition. The T_g recovers by about 16 deg with PCZ-2 for both concentrations of TPD. PCZ-3 shows the smallest recovery with 50% TPD. The higher T_g recovery in the case of PCZ-1, as compared to PCZ-2 and PCZ-3 could be attributed to its lower molecular weight and the large polydispersity.

As noted above, the T_g of PCZ (e.g., 178 °C for PCZ-3) is higher than that of BPAPC. The annealing temperatures used here are close to the T_g of BPAPC and far below that of PCZ. We did not use higher temperatures for annealing the PCZ composites because these would be close to the melting temperature of TPD. These being a homologous set of polymers, i.e., differing only in the nature of the side group, it can be expected that the T_g recovery would depend on the difference ΔT_{ann} between the T_g of the polymer and the annealing temperature. Figure 8a shows the variation of the extent of T_g recovery with ΔT_{ann}, for both BPAPC and PCZ in the same plot, after annealing (at 120, 130, and 140 °C) for 4 h. It is seen that with BPAPC and PCZ-3, which are similar in terms of molecular weight and polydispersity, there is a linear variation of T_g recovery with the ΔT_{ann}. It is also seen that the values for PCZ-2 are higher than those for PCZ-3. As discussed above, the lower molecular weight and the higher polydispersity lead to a higher T_g recovery. Thus, even when comparing the behavior of a homologous series, the relative M_w and its dispersity play a role in the T_g recovery, although the M_w's are fairly high. The variation of T_g recovery with ΔT_{ann} in Figure 8a can be expressed as (we are giving these equations to compare the slopes of the various curves in Figure 8a,b; see below)

$$T_{g(rec)} = 12.13 - 0.124\Delta T_{ann} \qquad R = 0.99 \qquad \text{for BPAPC and PCZ-3} \quad (2)$$

$$T_{g(rec)} = 23.59 - 0.2\Delta T_{ann} \qquad R = 0.96 \qquad \text{for PCZ-2} \quad (3)$$

Crystallinity of Phase-Separated TPD. The crystallinity of the phase-separated TPD was determined from the heat of fusion and X-ray diffraction. Here we refer to crystallinity as the weight percent of the TPD that crystallized out of the matrix. It is significant for a concentration of 50% TPD in the film with prolonged annealing. The results are given in Table 3 for the various compositions. Typical changes in the X-ray diffraction

TABLE 3: Crystallinity Calculated from DSC and X-ray Diffraction Measurements

	DSC crystallinity after annealing			X-ray crystallinity after annealing		
time (h)	120 °C	130 °C	140 °C	120 °C	130 °C	140 °C
			TPD/BPAPC: 40/60 wt %			
0		0	0	0.04	0.04	0.04
0.5		0	0.02	0.04	0.05	0.06
1		0.01	0.07	0.06	0.10	0.11
2		0.04	0.13	0.08	0.1	0.15
4		0.06	0.13	0.09	0.12	0.17
			TPD/BPAPC: 50/50 wt %			
0	0.03	0.03	0.03	0.04	0.04	0.04
0.5	0.04	0.04	0.07	0.05	0.08	0.11
1	0.06	0.07	0.09	0.06	0.1	0.19
2	0.09	0.10	0.13	0.14	0.18	0.23
4	0.18	0.27	0.3	0.16	0.23	0.25
			TPD/PCZ-1: 40/60 wt %			
0					0.08	0.08
0.5					0.09	0.1
1					0.10	0.11
2					0.13	0.15
4					0.16	0.16
			TPD/PCZ-2: 40/60 wt %			
0						0.06
0.5						0.07
1						0.086
2						0.072
4						0.076
			TPD/PCZ-2:50/50 wt %			
0	0	0	0			0.07
0.5	0.00	0.01	0.03			0.07
1	0.02	0.05	0.11			0.09
2	0.02	0.08	0.14			0.08
4	0.03	0.09	0.15			0.08
			TPD/PCZ-3: 40/60 (wt %			
0						0.06
0.5						0.08
1						0.07
2						0.08
4						0.08
			TPD/PCZ-3:50/50 (wt)%			
0	0	0	0			0.06
0.5	0	0.01	0.01			0.07
1	0.01	0.01	0.02			0.07
2	0.02	0.03	0.04			0.09
4	0.02	0.03	0.05			0.12

profile upon annealing are illustrated in Figure 9, for the TPD/BPAPC: 50/50 film, with annealing time for a temperature of 140 °C. Before annealing, no crystalline peak is seen; i.e., the TPD is molecularly dispersed and no aggregation has taken place to form crystals that could be detected by X-ray diffraction. After 0.5 h, the peaks due to TPD begin to appear. The crystalline peaks become more pronounced with annealing time. The intensity of these peaks increase significantly between 0.5 and 1 h. The crystallinities calculated from the DSC results and X-ray diffraction are shown in Figure 10a,b, respectively, for films with 50% TPD in BPAPC, with annealing temperature and time. It is seen that the values of the crystallinity from X-ray diffraction are in the same range as those derived from the DSC measurements, although the rate of change with time is different. This will be discussed below. It is seen from Table 3 that with 40% TPD, annealing at 120 °C did not yield a detectible endotherm for the small molecule, whereas the X-ray crystallinity is seen to be about 9%. However, even in this case, the DSC crystallinity is found to be as high as 13% with annealing at 140 °C, and with 50% TPD, it increases to nearly 30%. The X-ray crystallinity is comparable to the DSC measurements.

Figure 11 shows the crystallinity for the TPD/PCZ-3:50/50 film as measured by DSC for the three temperatures and by X-ray diffraction for the film annealed at 140 °C. It is realized that the values of crystallinity are very small, but these are shown here to compare with the case of TPD/BPAPC. The crystallinity in this case is far less than that observed in Figure 10 for the case of TPD/BPAPC. This can be attributed to the higher level of interaction between TPD and PCZ, as evidenced by the conformational energies and the IR frequency shifts, as well as the difference in the annealing temperature and the T_g of PCZ. As with the trend seen in Figure 10, the rate of change of crystallinity with time is different, as measured by DSC and X-ray diffraction.

Although the crystallinities from both methods are similar after annealing for 2 h, the rate of its change is higher with the X-ray measurement (Figure 10). In addition, the values level off after 2 h with the latter. Up to 2 h of annealing, the DSC crystallinity (H_{cr}) is lower. Although such a difference can be expected when comparing two different methods, it is also tempting to speculate its origin. As mentioned in the Experimental Section, the DSC crystallinity was calculated with reference to the heat of fusion of the 100% crystalline TPD. It was also noted that the melting point of the TPD in the composite was about 5 deg lower than that of the original value. It is then likely that the heat of fusion is also lowered when the TPD is dispersed in the polymer. The same trend is seen in Figure 11, for the TPD/PCZ-3 composite; i.e., the DSC crystallinity is lower than the results of the X-ray measurements.

Figure 8b shows the variation of the crystallinity of the phase-separated TPD as a function of ΔT_{ann}, the difference between the T_g of the polymer and the annealing temperature, after annealing (at 120, 130, and 140 °C) for 4 h. The DSC crystallinity is plotted here, to be consistent with Figure 8a, showing the variation of the T_g recovery. It is seen that the crystallinity of the phase-separated TPD decreases with an increase in ΔT_{ann}. The curve for PCZ-3 shows negligible crystallinity. The results shown in this figure can be fitted to a linear regression, with the following relationships:

$$H_{cr} = 35.69 - 0.6\Delta T_{ann} \qquad R = 0.99 \qquad \text{for BPAPC and PCZ-2} \quad (4)$$

$$H_{cr} = 10.62 - 0.15\Delta T_{ann} \qquad R = 0.98 \qquad \text{for PCZ-3} \quad (5)$$

Comparison of Figure 8a,b shows that the slope of the T_g recovery with ΔT_{ann} is the same (0.12) for BPAPC and PCZ-3 (eq 2). However, the variation of TPD crystallinity has a more pronounced slope for the case of BPAPC (0.6) than for PCZ-3 (0.15). The slopes of the T_g recovery and the crystallinity are similar for the case of PCZ-3 (see eqs 2−5). One would expect the variation of crystallinity of the phase-separated TPD to parallel the recovery of the T_g. We may rationalize the discrepancy in the case of BPAPC as follows:

The crystallinity of the phase-separated TPD is about 30% in the case of its composite with BPAPC, with annealing at 140 °C for 4 h. It is puzzling, however, that with such an increase in the crystallinity of the TPD, the recovery of the T_g is rather small. Though with a concentration of 50% TPD, the T_g of the BPAPC is reduced by 78 deg (Figure 2), the increase in the T_g is rather small (about 10 deg) when the crystallinity of the phase-separated TPD is close to 30%. Table 1 shows that there is a difference of 15 deg in the T_g between the composites with 40 and 50% TPD. Although even a difference of 10% in the concentration causes a decrease of 15 deg in the

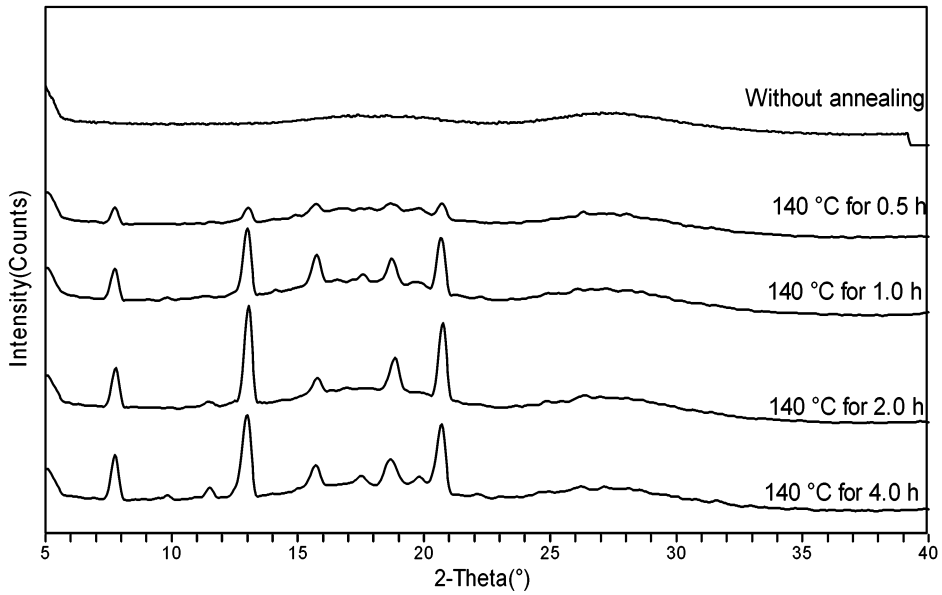

Figure 9. X-ray diffraction traces of a TPD/BPAPC film (50/50 wt %) annealed at 140 °C for various times.

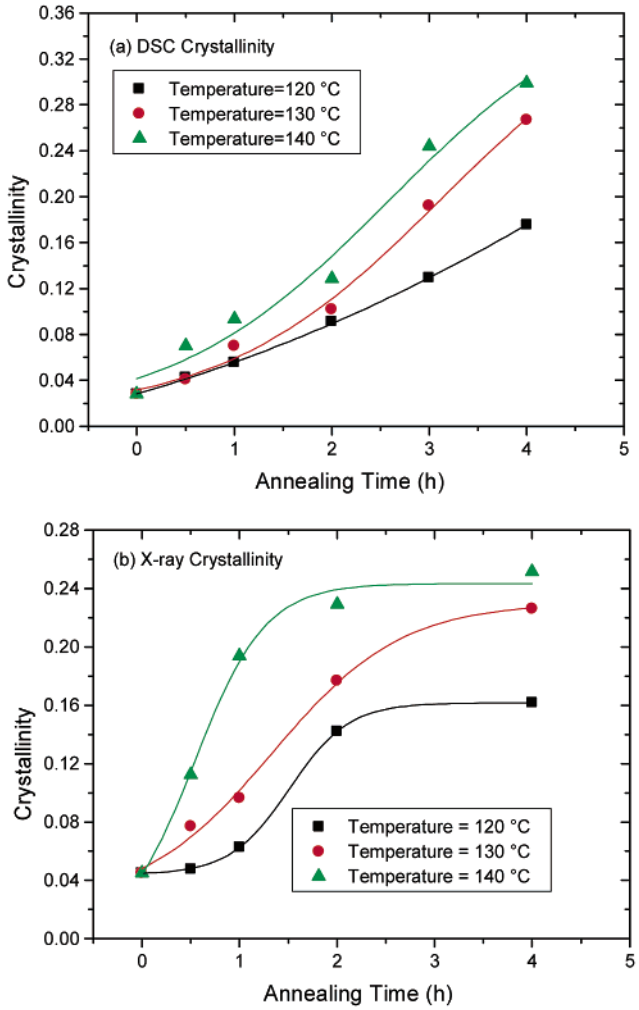

Figure 10. Crystallinity versus annealing time for TPD/BPAPC (50:50 wt %) films measured by (a) the DSC method (b) X-ray diffraction.

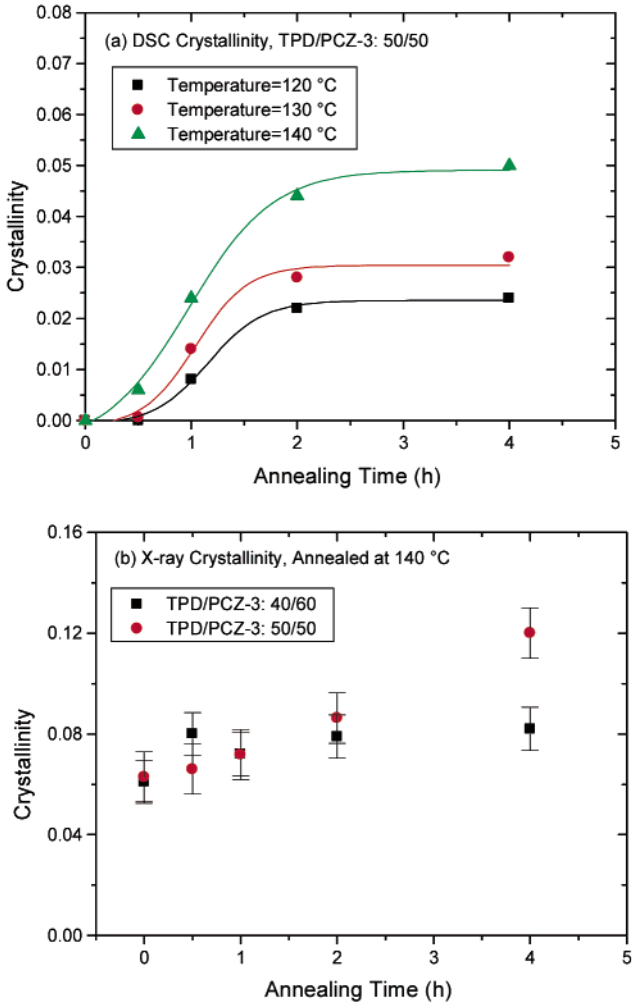

Figure 11. Crystallinity versus annealing time for TPD/PCZ-3 films measured by (a) the DSC method (b) X-ray diffraction.

as-prepared films, the T_g recovery is small even with a crystallinity of 30%. Both optical microscopy and SEM showed a wide distribution of crystal sizes, ranging from 1 to 200 μm in the case of TPD/BPAPC. It is likely that the small submicron crystals of TPD actually act to plasticize; i.e., a competing process occurs in which the phase separation of TPD increases the T_g, whereas this increase is partially offset by the small crystals of TPD acting to depress the T_g. As mentioned above (see Figure 7), the transitions are rather broad for the annealed films.

The recovery of the T_g upon annealing and the resultant TPD crystallinity are in concert with each other with PCZ-2 and PCZ-3. As noted from Table 1, the difference in the T_g between 40 and 50% concentrations of TPD in PCZ-2 and PCZ-3 in the as-prepared films is only about 5°. In this case, the crystals were needlelike, ranging in length from 50 to 200 μm. Comparing Figures 10 and 11, the initial rate of increase in X-ray crystallinity for TPD/BPAPC is higher than that of the TPD/PCZ. The higher flexibility of BPAPC, as well as the difference between the annealing temperature and the T_g of the polymer lead to enhanced rate of crystallization of TPD.

It was mentioned in the Introduction that crystallization of TPD would lead to charge trapping. Its effect on the residual potential has been discussed by Scharfe[22] and Schaffert.[42] When the photoreceptor is exposed to light, the electrical potential undergoes an initial rapid decay, followed by a relatively slow decay. The potential at the point where the slow decay begins is the residual potential (V_r). A low residual potential is desirable because of the greater voltage contrast that is possible. To illustrate the effect of TPD crystallization on V_r, a photoreceptor device using 50:50 wt % of TPD and BPAPC or PCZ-3 was annealed at 140 °C, for 2 min and 2 h. Though annealing for 2 min did not cause any change, for the device with BPAPC, the V_r increased by a factor of 4.3 upon annealing for 2 h, and by a factor of 1.9 for the device using PCZ-3.

Conclusions

The current studies on the TPD/polycarbonate composites show that the glass transition temperature of the polycarbonate is reduced significantly in the presence of the TPD. The depression of the T_g is more pronounced in the case of the PCZ polycarbonate, which is conformationally more restricted. This is in part due to the large reduction in the conformational energy of the TPD/PCZ pair relative to that with BPAPC. Molecular modeling shows that the biphenyl segment of TPD stacks with one of the phenyl groups of the polycarbonate. IR spectra show shifts of aromatic group absorption bands to lower frequencies when the polycarbonates are mixed with TPD, indicating molecular interactions involving the phenyl groups. The extent of the shift is more in the case of PCZ. The frequency shifts follow the same trend as the depression of the T_g. Annealing induces crystallization of the TPD due to phase separation and leads to a recovery of the T_g of the host polymer. The crystallization and the T_g recovery were found to be small in the case of PCZ based composites relative to those with BPAPC, annealed at the same temperatures. This is attributed to the lower molecular flexibility of PCZ as compared to BPAPC.[26,27] The extent of T_g recovery does not accord with the crystallinity of phase-separated TPD in the case of BPAPC, perhaps due to the plasticization by submicron crystals of TPD. Although the extent of the T_g recovery depends on the difference ΔT_{ann} between the T_g of the host polymer and the annealing temperature, the differences in the molecular weight and its distribution plays a role, even with a homologous series.

Acknowledgment. This work was supported by the Natural Sciences and Engineering Research Council of Canada (NSERC), Xerox Research Centre of Canada (XRCC), and the Xerox Corp., USA. We thank Dr. Mike Day for providing access to the DSC facility at the National Research Council of Canada.

References and Notes

(1) Borsenberger, P. M.; Weiss, D. S. *Organic Photoreceptors for Xerography*, Marcel Decker: New York, 1998. Melnyk, A. R.; Pai, D. M. Hard Copy and Printing Materials, Media and Process. *Proc. SPIE* **1990**, *1253*, 141.

(2) Stolka, M.; Yanus, J. F.; Pai, D. M. *J. Phys. Chem.* **1984**, *88*, 4707.

(3) Borsenberger, P. M. *J. Appl. Phys.* **1990**, *68*, 6263.

(4) Lin, L.-B.; Jenekhe, S. A.; Borsenberger, P. M. *Appl. Phys. Lett.* **1996**, *69*, 3495.

(5) Yuh, H.-J.; Pai, D. M. *Philos. Mag. Lett.* **1990**, *62*, 61.

(6) Yuh, H.-J.; Pai, D. M. Hard Copy and Printing Materials, Media and Process. *Proc. SPIE* **1990**, *1253*, 162.

(7) Yuh, H.-J.; Pai, D. M. *Mol. Cryst. Liq. Cryst*, **1990**, *183*, 217.

(8) Pai, D. M. In *Frontiers of Polymer Research*; Prasad, P. N.; Nigam, J. K. Eds.; Plenum Press: New York, 1991; p 315.

(9) Yuh, H.-J.; Pai D. M. *J. Imaging Sci. Tech*. **1992**, *36*, 477.

(10) Mishra, S.; Pai, D. M.; Yanus, J.; Yuh, H− J.; Antoniadis, H. *Proc. Int. Congr. Adv. Non-Impact Print. Technol*. **1993**, p 635.

(11) Yamamori, A.; Adachi, C.; Koyama, T.; Taniguchi, Y. *J. Appl. Phys.* **1999**, *86*, 4369.

(12) Anderson, J. D.; McDonald, E. M.; Lee, P. A.; Anderson, M. L.; Ritchie, E. L.; Hall, H. K.; Hopkins, T.; Mash, E. A.; Wang, J.; Padias, A.; Thayumanavan, S.; Barlow, S.; Marder, S. R.; Jabbour, G. E.; Shaheen, S.; Kippelen, B.; Peyghambarian, N.; Wightman, R. M.; Armstrong, N. R. *J. Am. Chem. Soc.* **1998**, *120*, 9646.

(13) Mattoussi, H.; Murata, H.; Merritt, C. D.; Iizumi, Y.; Kido, J.; Kafafi, Z. H. *J. Appl. Phys.* **1999**, *86*, 2642.

(14) Py, C.; Roth, D.; Lévesque, I.; Stapledon, J.; Donat-Bouillud, A. *Synth. Met.* **2001**, *122*, 225.

(15) Savvate'ev, V.; Friedl, J. H.; Zou, L.; Christensen, K.; Oldham, W.; Rothberg, L. J.; Chen-Esterlit, Z.; Kopelman, R.; Shinar, J. *Synth. Met.* **2001**, *121*, 1713.

(16) Shaheen, S. E.; Jabbour, G. E.; Morrell, M. M.; Kawabe, Y.; Kippelen, B.; Peyghambarian, N.; Nabor, M.-F.; Schlaf, R.; Mash, E. A.; Armstrong, N. R. *J. Appl. Phys.* **1998**, *84*, 2324.

(17) Pai, D. M.; Yanus, J. F.; Stolka, M. *J. Phys. Chem.* **1984**, *88*, 4714.

(18) Stolka, M.; Abkowitz, M. A. *Mater Res Soc. Symp Proc*. **1992**, *277*, 15

(19) Santerre, F.; Bedja, I.; Dodelet, J. P.; Sun, Y.; Lu, J.; Hay, A. S.; D'Iorio, M. *Chem. Mater*. **2001**, *13*, 1739.

(20) Kaplan, S. *Macromolecules* **1993**, *26*, 1060.

(21) Smith, P. F.; Gerroir, P.; Xie, S.; Hor, A. M.; Popovic, Z. *Langmuir* **1998**, *14*, 5946.

(22) Scharfe, M. *Electrophotography Principles and Optimization*; John Wiley & Sons: New York, 1984.

(23) Normandin, S. E.; Sullivan, D. P.; Willnow, H.; Carmichael, W.; Thomsen, K. V.; Bergfjord, J. A. U.S. Patent 5,492,785, 1996.

(24) Kemmesat, P. D.; Neely, J. K.; Randolph, C. M.; Srinivasan, K. R. U.S. Patent 6,001,523, 1999.

(25) Sugimura, H.; Nakamura, T. Jpn. Kokai Tokkyo Koho JP 1356501, 2001; *Chem Abstr. 136*, 61503.

(26) Sundararajan, P. R. *Macromolecules* **1989**, *22*, 2149.

(27) Sundararajan, P. R. *Macromolecules* **1993**, *26*, 344.

(28) Kennedy, A. R.; Ewen Smith, W.; Tackley, D. R.; David, W. I. F.; Shankland, K.; Brown, B.; Teat, S. J. *J. Mater. Chem*. **2002**, *12*, 168.

(29) Madkour, T. M. In *Polymer Data Handbook*; Mark, J. E. Ed.; Oxford University Press: New York, 1999; p 363.

(30) Alexandru. L.; Zamin, J.; Sundararajan, P. R. *J. Appl. Polym. Sci*. **1991**, *43*, 2259.

(31) Drappel, S.; Sundararajan, P. R.; Rudin, A. *Poymer* **1997**, *38*, 1259.

(32) Tuteja, B.; Khan, F.; Sundararajan, P. R. To be published.

(33) Taylor, M. G.; Sundararajan, P. R. *Macromolecules* **1990**, *23*, 2602.

(34) Kelley, F. N.; Bueche, F. *J. Polym. Sci*. **1961**, *50*, 549.

(35) Couchman, P. R.; Karasz, F. E. *Macromolecules* **1978**, *11*, 117.

(36) Fox, T. G. *Bull. Am. Phys. Soc*. **1956**, *1*, 123.

(37) O'Brien, D. F.; Burrows, P. E.; Forrest, S. R.; Koene, B. E.; Loy, D. E.; Thompson, M. E. *Adv. Mater*. **1998**, *10*, 1108.

(38) Shirota, Y.; Okumoto, K.; Inada, H. *Synth. Met*. **2000**, *111*−*112*, 387.

(39) Noda, I.; Dowrey, A. E.; Marcott, C. In *Physical Properties of Polymers Handbook*; Mark. J. E., Ed.; Am. Inst. Phys.: New York, 1996; p 291.

(40) Schmidt, P.; Dybal, J.; Turska, E.; Kulczycki, A. *Polymer* **1991**, *32*, 1862.

(41) Heymans N. *Polymer* **1997**, *38*, 3435.

(42) Schaffert, R. M. *Electrophotography*; Focal Press: London, 1980; Chapter 2.